Understanding the Nature and Properties of Hydrogen-Hydrogen Bonds: The Stability of a Bulky Phosphatetrahedrane as a Case Study

Martin-Louis Y. Riu,† Giovanni Bistoni,*,‡ and Christopher C. Cummins*,†

†*Department of Chemistry, Massachusetts Institute of Technology, Cambridge, MA 02139, USA*

‡*Max-Planck-Institut für Kohlenforschung, Stiftstrasse 34-36, D-45470 Mülheim an der Ruhr, Germany*

E-mail: giovanni.bistoni@kofo.mpg.de; ccummins@mit.edu

Abstract

Recently, the first mixed C/P phosphatetrahedranes $(^t\mathrm{BuC})_3\mathrm{P}$ and $(^t\mathrm{BuCP})_2$ were reported. Unlike $(^t\mathrm{BuCP})_2$, $(^t\mathrm{BuC})_3\mathrm{P}$ exhibits remarkable thermal stability, which can be partially attributed to a network of nine hydrogen-hydrogen bonds (HHBs) localized between the *tert*-butyl substituents. The stabilizing contribution arising from this network of HHBs were obtained from local energy decomposition (LED) analysis calculated at the domain-based local pair natural orbital CCSD(T) (DLPNO-CCSD(T)) level of theory. These calculations suggest that each HHB contributes approximately −0.7 kcal/mol of stabilization; however, the net stabilization energy likely lies between −0.25 and −0.5 kcal/mol due to steric repulsion. Spatial analysis of the London dispersion energy via a dispersion interaction density (DID) plot reveals that the DID surface is localized at key C−H groups involved in HHBs, consistent with London dispersion interactions predominantly arising from HHBs. In addition, we present a computed mechanism that supports a phosphinidenoid species as a key reaction intermediate in the synthesis of $(^t\text{BuC})_3\text{P}$.

Introduction

The significant strain and ensuing high reactivity of tetrahedranes have attracted the attention of chemists for decades. In 1978, Maier and co-workers successfully isolated tetra-*tert*-butyl tetrahedrane ($(^t\text{BuC})_4$), a tetrahedrane with a core composed of only carbon atoms.[1] In this seminal study, the authors found that the isolated tetrahedrane exhibits remarkable thermal stability and attributed this property to the accumulation of four sterically demanding substituents that effectively enclose the highly reactive tetrahedrane core. In order to expose the tetrahedrane core, the hydrogen atoms of the *tert*-butyl substituents must be forced into close contact, a phenomenon that was termed the "corset effect" by Maier. Indeed, early attempts to prepare tetrahedranes with phenyl and methyl substituents were unsuccessful, even under matrix isolation conditions.[2–6] However, it was later shown by Sekiguchi and co-workers that tetrahedrane derivatives with less bulky groups could be prepared by incorporating strongly σ-donating and π-accepting trimethylsilyl substituents,[7–9] which have a stabilizing effect on strained organic systems.[10–12]

In 2003, Bader proposed that the stability of $(^t\text{BuC})_4$ is partially accounted for by a network of 18 hydrogen-hydrogen bonds (HHB), which imparts significant stabilization energy on the tetrahedrane through London dispersion (LD) interactions.[13] In fact, atoms in molecules (AIM)[14,15] analysis suggests that the network of HHBs found in the T-symmetric structure, the lowest energy conformer of $(^t\text{BuC})_4$,[16] contributes 13.2 kcal/mol of stabilization.[13] However, a more recent computational analysis (B3LYP/6-31G(d,p) level of theory) estimates that the stabilization energy arising from dispersion interactions is closer to 3.1 kcal/mol using an isodesmic reaction.[17] Despite significant debate over the nature and existence of hydrogen-hydrogen bonds,[18–27] these interactions have been identified in a number of other systems. For example, HHBs have been examined in alkane complexes[28–30] and a direct relationship between the number of HHBs and the boiling points of linear alkanes, as well as the stability of the complexes, was found.[31] Additionally, homopolar hydrogen-hydrogen interactions have been identified in main group hydrides[32–34] and, in particular, shown to have a significant stabilizing effect on the solid state structures of alkali-metal amidoboranes used for hydrogen storage.[35,36] However, whether these interactions are net attractive or repulsive is still a matter of debate.[37] Furthermore, Garcia and co-workers have even demonstrated that the coordination geometry of a transition-metal complex may be affected by HHBs between ligand substituents and free hydrocarbons.[38]

Recently, the first mixed phosphatetrahedranes, $(^t\mathrm{BuC})_3\mathrm{P}$[39] and $(^t\mathrm{BuCP})_2$,[40] were reported. The successful isolation of these compounds is consistent with our chemical intuition that higher main group elements better accommodate acute bond angles[41] and, consequently, have a stabilizing effect on the tetrahedrane core.[42] The synthesis of $(^t\mathrm{BuC})_3\mathrm{P}$ required the development of novel reaction chemistry and was prepared via the dehydrohalogenation of a cyclopropenyl-substituted hydro(fluoro)phosphine. We have proposed that this reaction generates an unsaturated phosphorus center that closes with the neighboring olefin to form the target molecule, though this reaction has yet to be thoroughly investigated in mechanistic detail.

We found that $(^t\mathrm{BuC})_3\mathrm{P}$ exhibits remarkable thermal stability, unlike $(^t\mathrm{BuCP})_2$, which decomposes above −32 °C when isolated. This suggests that the incorporation of bulky *tert*-butyl substituents likely also plays a critical role in kinetically stabilizing the isolated phosphatetrahedranes. Analysis of NBO second-order perturbation energies reveals that the donation of the C−C and C−P bonds of $(^t\mathrm{BuC})_3\mathrm{P}$ into the $\mathrm{C{-}C}_{^t\mathrm{Bu}}$ antibonds plays a critical role in the stabilization of the tetrahedrane.[42] This analysis suggests that the *tert*-butyl substituents provide as much as 16 kcal/mol of stabilization through this interaction. While it may not be the dominating factor, we propose that $(^t\mathrm{BuC})_3\mathrm{P}$ is also stabilized by a network of HHBs through LD forces.

London dispersion is a pure electron correlation effect; therefore, this network interactions would be best described by highly accurate first principle computational methods, such as the coupled-cluster method with singles, doubles, and perturbative triples excitations (CCSD(T)).[43] However, these methods are often prohibitively computationally expensive for large systems. Generally, density functional theory (DFT) is employed when analyzing molecular systems of this size, but it does not adequately describe weak interactions.[44,45] A force field correction, such as Grimme's popular −D3 correction,[46] is commonly included to better account for non-covalent interactions, but the dispersion energies obtained from these calculations are highly functional dependent.[47] The domain-based local pair natural orbital variant of CCSD(T) (DLPNO-CCSD(T)) was recently reported and it allows for coupled-cluster calculations be performed on large systems while retaining its high accuracy.[48,49] Moreover, a local energy decomposition (LED) scheme for DLPNO-CCSD(T) was developed and may be employed to analyze and quantify non-covalent interactions.[43,50–52]

Herein, we describe the nature and properties of hydrogen-hydrogen bonds found in bulky phosphatetrahedranes at the DLPNO-CCSD(T) level of theory. A LED scheme was used to extract the dispersion energy found between the substituents. From these values, we are able to comment the stabilization energy imparted by HHBs found between bulky substituents of selected phosphatetrahedranes. Additionally, we present a computed mechanism that is consistent with $(^t\mathrm{BuC})_3\mathrm{P}$ formation via a transiently formed cyclopropenyl-substituted halophosphide anion.

Computational Details

All calculations were performed using a development version of the ORCA quantum chemistry package based on version 4.2.[53,54] Geometry optimizations and harmonic frequencies calculations for $(^t\mathrm{BuC})_3\mathrm{P}$, methane dimer and trimer, isobutane dimer and trimer, $(^t\mathrm{Bu})_2(\mathrm{H})\mathrm{C}_3\mathrm{P}$, $(^t\mathrm{Bu})_2(\mathrm{Me})\mathrm{C}_3\mathrm{P}$, $(^t\mathrm{Bu})_2(\mathrm{Et})\mathrm{C}_3\mathrm{P}$, and $(^t\mathrm{Bu})_2(^i\mathrm{Pr})\mathrm{C}_3\mathrm{P}$ were carried out using density functional theory (DFT) with the TPSS-D3 functional[46,55] in conjunction with the def2-TZVP orbital basis set[56] and def2/J auxiliary basis sets.[57] The Becke-Johnson damping parameters were used in the −D3 correction.[58,59] Geometry optimizations and frequencies calculations for $[(HC)_3P(Cl)]^-$, $(HC)_3P$, and the associated transition state were carried out using DFT at the B3LYP-D3/ma-def2-TZVP(-f) level of theory[46,56,58] with a THF CPCM solvation model[60] and def2/J auxiliary basis sets.[57] The Becke-Johnson damping parameters were used in the −D3 correction.[58,59] Single point energies for all structures were calculated using the domain-based local pair natural orbital coupled-cluster method with singles, doubles, and perturbative triples excitation (DLPNO-CCSD(T))[61] using TightPNO settings[62] and the cc-pVQZ basis set.[63] London dispersion energies were quantified using the Local Energy Decomposition (LED) scheme.[50] The contribution of the triples correction to the London dispersion was estimated as detailed in Ref. 64 and 52. Intrinsic bond orbitals (IBOs)[65] were generated using IboView.[66]

Results and Discussion

Methane Dimer

When investigating the effect of hydrogen-hydrogen bond interactions between substituents in $(^t\mathrm{BuC})_3\mathrm{P}$ and its contribution to the stability of the molecule, it is important to consider the opposing contribution from steric repulsion. The balance of these two effects dictates whether these non-covalent interactions have an overall stabilizing effect.[30,67,68] Hence, before beginning our discussion on the effect of HHB interactions in $(^t\mathrm{BuC})_3\mathrm{P}$, it is useful to consider the dissociation energy profile for the simplest system containing a HHB interaction, that is, the methane dimer in the conformation shown in Figure 1. For this system, the interaction between the two methane molecules becomes attractive when the H−H distance (highlighted in red) is greater than 2.2 Å. The energy reaches a minimum at ca. 2.6 Å and increases slowly upon increasing the distance of separation. Note that, in contrast to the total energy, the attractive LD energy always increases in magnitude for shorter H—H contacts. However, for H—H distances smaller than 2.2 Å, the repulsive contributions to the interaction (e.g. steric repulsion) dominate over the dispersion energy. This analysis suggests that H—H contacts with internuclear distances below 2.2 Å are net repulsive while those with H—H distance between 2.3 and 2.8 Å are net attractive.

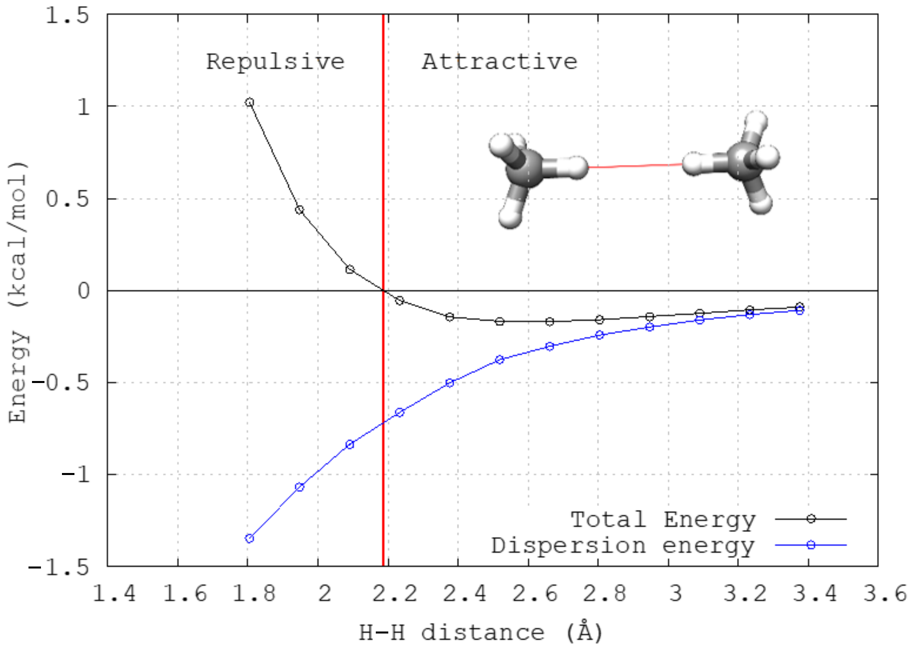

Figure 1: Dissociation Energy Profile for the Methane Dimer. The vertical red line denotes the H—H bond distance at which the interaction changes sign (ca. 2.2 Å). Values for energy (kcal/mol) were obtained at the DLPNO-CCSD(T) level of theory using TightPNO settings and the cc-pVQZ basis set.

London Dispersion Interactions in $(^t\mathrm{BuC})_3\mathrm{P}$

Depicted in Figure 2 is the DFT optimized structure of $(^t\mathrm{BuC})_3\mathrm{P}$ (TPSS-D3/def2-TZVP level of theory). Note that the staggered conformation of the *tert*-butyl substituents in $(^t\mathrm{BuC})_3\mathrm{P}$ are consistent with the favorable $T_d \to T$ distortion found for tetra-*tert*-butyl tetrahedrane.[16,69] Roughly speaking, 9 HHBs with internuclear distances that lie between 2.3 and 2.6 Å can be identified in this system (highlighted in red in Figure 2A). This depicted network of HHBs closely resembles the nine intramolecular bond paths between pairs of adjacent *tert*-butyl hydrogen atoms revealed by topological analysis of the electron density (B3LYP-D3/6-31G**) for $(^{t}\text{BuC})_3\text{P}$.[39] In order to quantify the stabilization energy associated with the network of HHBs, the phosphatetrahedrane was divided into four fragments, one for each *tert*-butyl group and one for the phosphatetrahedrane core (Figure 2B). The LD interaction between each pair of *tert*-butyl groups was found to be -2.2 kcal/mol. Hence, the overall stabilizing effect originating from LD forces acting between the *tert*-butyl groups is -6.6 kcal/mol, suggesting that the average LD energy contribution associated with a HHB is -0.7 kcal/mol. This value is of course slightly overestimated because we are assuming that LD originates exclusively from those 9 HHBs. Additionally, the stabilization energy imparted by covalent-like charge delocalization, which has been shown to have a minor contribution to the overall HHB stabilization energy, is not accounted for.[29,70] Nevertheless, it is roughly consistent with that obtained for the methane dimer when the HHB distance is ca. 2.2 Å and Bader's estimate that, on average, each of the 18 HHB found in the T-symmetric structure of $(^{t}\text{BuC})_4$ contributes approximately 0.8 kcal/mol to the structure's stabilization.[13] For reference, the intramolecular hydrogen-hydrogen bond found for the "*in-in*" conformer of *o*-xylene contributes as much as 4.8 kcal/mol of stabilization based on the recently developed IQA (Interacting Quantum Atoms)[71]-based FAMSEC (real space fragment attributed molecular system energy change)[72] approach.[26]

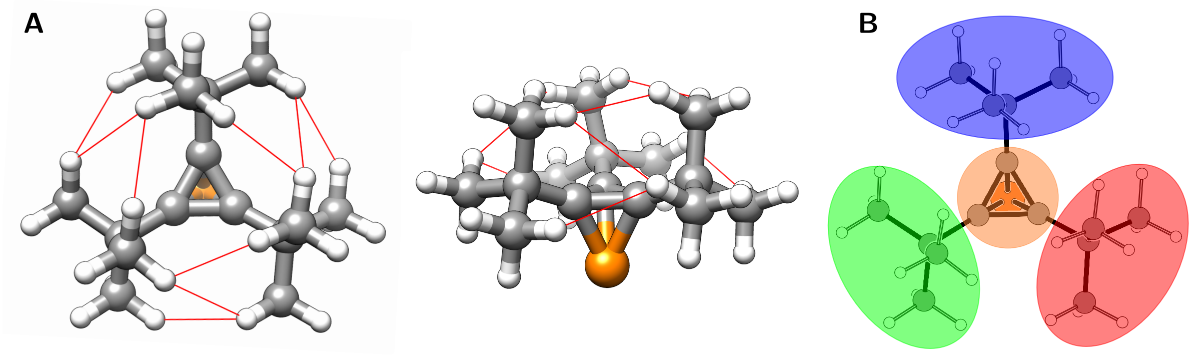

Figure 2: A) Structure of $(^{t}\text{BuC})_3\text{P}$ (top view, left; side view, right). The HHB contacts associated with the interaction of neighbouring *tert*-butyl groups are highlighted in red and all lie between 2.3 and 2.6 Å. B) Fragmentation pattern of $(^{t}\text{BuC})_3\text{P}$ for LED analysis with colored ellipses denoting different fragments.

To verify these findings, we have analyzed an intermolecular model system constituting two molecules of isobutane placed exactly in the same position of a pair of *tert*-butyl groups in (^{t}BuC)$_3$P. The so-called Dispersion Interaction Density (DID) [51,73] plot for this system is depicted in Figure 3. This plot provides a spatial analysis of the London dispersion energy extracted at the DLPNO-CCSD(T)/LED level and integration of the corresponding DID surface provides the exact value of the LD energy.

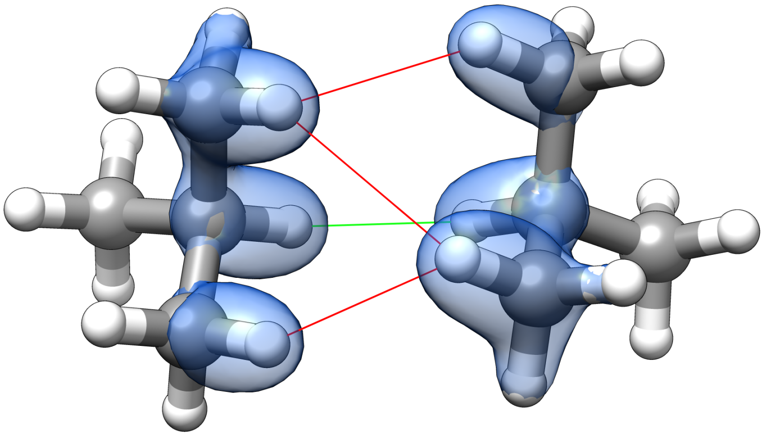

Figure 3: Spatial Analysis of the London Dispersion Energy. Dispersion Interaction Density (DID) plot for the interaction of two molecules of isobutane placed exactly in the same position as the *tert*-butyl groups in (^{t}BuC)$_3$P. "Attractive" HHB contacts are highlighted in red, "repulsive" contacts are emphasized in green. The isovalue for the DID surface is 0.1 kcal/mol.

Interestingly, the DID surface is mainly localized around the key C−H groups involved in the hydrogen-hydrogen bonds. Additionally, two C−H groups exhibit more extended DID surfaces than the others. This effect originates from the fact that these C−H groups are involved in the formation of two HHBs. This was also confirmed by a detailed analysis of the double excitation contributions constituting the LD dispersion energy. This finding demonstrates that the stabilizing LD energy in this system originates mainly from H−H contacts.

Four HHBs were found for this model system, three corresponding to the interaction of methyl groups (the HHB distance is greater than 2.2 Å) and one representing the H−H interaction involving the tertiary carbons (the HHB distance is 2.1 Å). The overall LD energy for this system is −3.3 kcal/mol. Hence, as a rule of thumb, we can conclude that each H−H contact contributes, on average, −0.7 kcal/mol to the overall LD energy. This is consistent with the discussion above. However, it is worth stressing that steric repulsion will significantly reduce the net stabilizing contribution association with a given HHB. This aspect is discussed in the next section.

The Balance Between London Dispersion and Steric Repulsion

Depicted in Figure 4 (left) is an intermolecular model system consisting of three interacting isobutane molecules placed exactly in the same position of the *tert*-butyl groups in $(^t\mathrm{BuC})_3\mathrm{P}$. The total association energy of the system, *i.e.*, the difference between the energy of the adduct and that of the three isobutane molecules placed at an infinite distance of separation, is −4.3 kcal/mol. Using the LED scheme, this number can be exactly decomposed into a contribution coming from the non-dispersive components of the interaction (in LED these are electronic preparation, electrostatics, exchange and non-dispersive correlation) and a contribution coming from the LD energy. The sum of all non-dispersive contributions is repulsive and amounts to +5.9 kcal/mol, whilst the LD energy amounts to −10.4 kcal/mol. Hence, this system is effectively held together by LD forces originating from 12 H−H contacts and the average contribution of each HHB to the overall LD energy is −0.9 kcal/mol.

If this system is simplified by replacing all methyl groups with hydrogens, as depicted in Figure 4 (right), an unstable structure with an association energy +0.3 kcal/mol is obtained. This is consistent with the methane dimer model discussed earlier. In fact, the simplified system features only 3 H−H contacts, which all exhibit internuclear distances below the threshold of 2.2 Å. The total LD contribution is fairly large and amounts to −2.9 kcal/mol. However, the repulsive contributions to the interaction sum up to +3.2 kcal/mol, making the overall interaction energy repulsive.

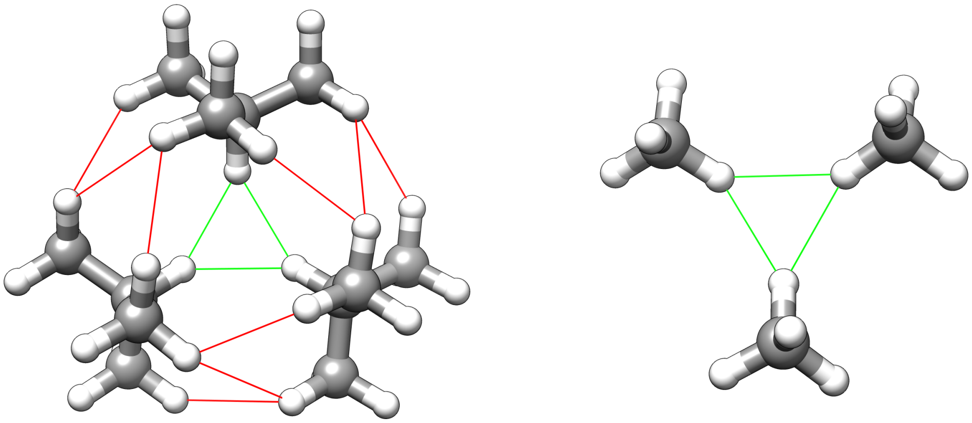

Figure 4: Intermolecular Model System. Left: the interaction of three molecules of isobutane placed exactly in the same position as the *tert*-butyl groups in $(^t\mathrm{BuC})_3\mathrm{P}$. Right: the interaction of three methane molecules in the same position.

Substituents Effects on the Dispersion Interactions in $(^t\mathrm{BuC})_3\mathrm{P}$

The network of HHBs found in $(^t\mathrm{BuC})_3\mathrm{P}$ was further investigated by systematically replacing one of the three *tert*-butyl substituents with a hydrogen ($(^t\mathrm{Bu})_2(\mathrm{H})\mathrm{C}_3\mathrm{P}$), methyl ($(^t\mathrm{Bu})_2(\mathrm{Me})\mathrm{C}_3\mathrm{P}$), ethyl ($(^t\mathrm{Bu})_2(\mathrm{Et})\mathrm{C}_3\mathrm{P}$), and isopropyl group ($(^t\mathrm{Bu})_2(^i\mathrm{Pr})\mathrm{C}_3\mathrm{P}$). The DFT-optimized structures (TPSS-D3/def2-TZVP level of theory) are depicted in Figure 5 and the HHBs with internuclear distances shorter than 2.8 Å are highlighted in red. Interestingly, $(^t\mathrm{Bu})_2(\mathrm{H})\mathrm{C}_3\mathrm{P}$, $(^t\mathrm{Bu})_2(\mathrm{Me})\mathrm{C}_3\mathrm{P}$, and $(^t\mathrm{Bu})_2(^i\mathrm{Pr})\mathrm{C}_3\mathrm{P}$ adopt C_s-symmetric structures, which results in fewer, but shorter, hydrogen-hydrogen bonds. This contrasts the orientation of the *tert*-butyl substituents found for the lowest energy conformers of $(^t\mathrm{Bu})_2(\mathrm{Et})\mathrm{C}_3\mathrm{P}$, $(^t\mathrm{BuC})_3\mathrm{P}$, and $(^t\mathrm{BuC})_4$.[16] It is important to note that while the T_d-symmetric structure of $(^t\mathrm{BuC})_4$ leads to greater stabilization from dispersion interactions between the *tert*-butyl substituents, calculations suggest that the T-symmetric is lower in energy due to stabilization of the tetrahedrane core.[13]

In order to quantify the dispersion energy found between each substituent of the phosphatetrahedrane derivatives discussed above, the phosphatetrahedranes were broken up into four fragments – two for the *tert*-butyl groups, one for the tetrahedrane core, and one for

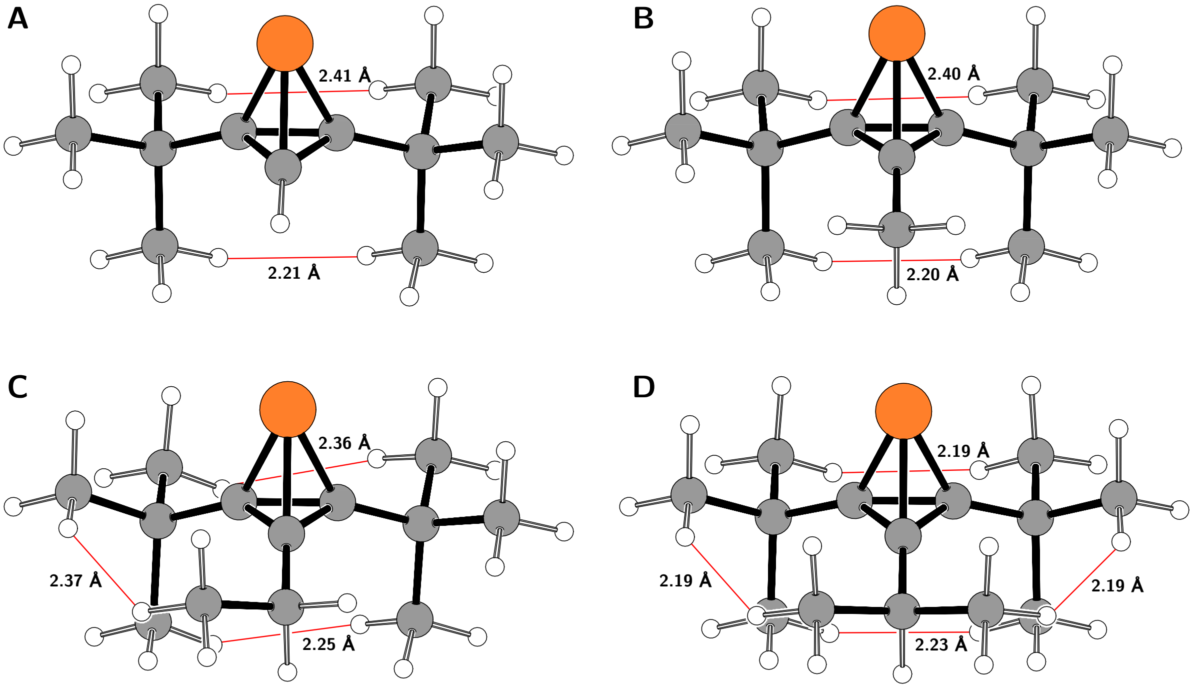

Figure 5: Optimized Structures of Bulky Phosphatetrahedrane Derivatives. **A**, **B**, **C**, and **D** depict the optimized structures of the $(^{t}\mathrm{Bu})_2(\mathrm{H})\mathrm{C}_3\mathrm{P}$, $(^{t}\mathrm{Bu})_2(\mathrm{Me})\mathrm{C}_3\mathrm{P}$, $(^{t}\mathrm{Bu})_2(\mathrm{Et})\mathrm{C}_3\mathrm{P}$, and $(^{t}\mathrm{Bu})_2(^{i}\mathrm{Pr})\mathrm{C}_3\mathrm{P}$, respectively. HHBs with internuclear distances of less than 2.8 Å are highlighted in red.

H−, Me−, Et−, and ^{i}Pr− groups. It was found that the total energy arising from dispersion interactions between substituents in $(^{t}\mathrm{Bu})_2(\mathrm{H})\mathrm{C}_3\mathrm{P}$, $(^{t}\mathrm{Bu})_2(\mathrm{Me})\mathrm{C}_3\mathrm{P}$, $(^{t}\mathrm{Bu})_2(\mathrm{Et})\mathrm{C}_3\mathrm{P}$, and $(^{t}\mathrm{Bu})_2(^{i}\mathrm{Pr})\mathrm{C}_3\mathrm{P}$ amounts to −2.0, −3.2, −4.0, and −5.2 kcal/mol, respectively (c.f. −6.6 for $(^{t}\mathrm{BuC})_3\mathrm{P}$). Considering the relatively short hydrogen-hydrogen bond lengths found in the optimized structures presented in Figure 5, it is important to note that steric repulsion may be significantly minimizing the stabilization effect arising from LD forces.

Computed Pathway of $(\mathrm{HC})_3\mathrm{P}$ Formation

Treatment of cyclopropenyl-substituted hydro(fluoro)phosphine $(^{t}\mathrm{BuC})_3\mathrm{P(F)H}$ with a strong, bulky base, such as lithium 2,2,6,6-tetramethylpiperidide (LiTMP), results in clean formation of $(^{t}\mathrm{BuC})_3\mathrm{P}$ (Figure 6).[39] It was proposed that the cyclopropenyl-substituted fluorophosphide $[(^{t}\mathrm{BuC})_3\mathrm{P(F)}]^-$ is transiently generated upon deprotonation of $(^{t}\mathrm{BuC})_3\mathrm{P(F)H}$ by LiTMP and that the anion reacts with the neighboring olefin to form $(^{t}\mathrm{BuC})_3\mathrm{P}$ with concomitant elimination of halide. Related phosphorus anions have been referred to as phosphinidenoids, in analogy to carbenoids.[74] Bulky transition-metal-stabilized phosphinidenoids have been isolated and characterized; however, [2+1]-cycloaddition reactivity of these species appears to be limited to heteronuclear π-systems, such as ketones and imines.[75,76]

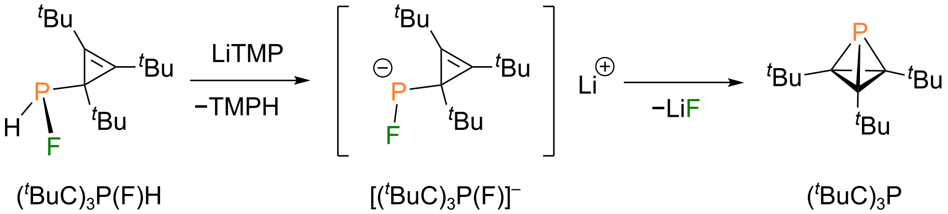

Figure 6: Synthesis of Tri-*tert*-butyl Phosphatetrahedrane ($(^tBuC)_3P$).[39]

Quantum chemical calculations were employed to elucidate the mechanism of $(^tBuC)_3P$ formation. Geometries were optimized at the ma-def2-TZVP(-f)/B3LYP-D3BJ, CPCM(THF) level of theory and the Gibbs free enthalpies ($T = 298.15$ K) were obtained using single point energies calculated at the DLPNO-CCSD(T)/aug-cc-pVDZ, CPCM(THF) level of theory. The results are summarized in Figure 7A; note that the parent phosphatetrahedrane and $[(HC)_3P(Cl)]^-$ were used in this model system. A transition state, consisting of concerted addition of the cyclopropenyl π-bond to the two-coordinate phosphorus center and simultaneous elimination of chloride, was located on the potential energy surface. The calculations suggest that the model reaction proceeds with a very low energetic barrier of +5.7 kcal/mol and that formation of $(HC)_3P$ is thermodynamically favorable by 20.2 kcal/mol, showing that this reaction is accompanied by significant driving force.

Further insight into the reaction mechanism was gained by means of intrinsic bond orbitals (IBOs).[65] Visualization of electron flow via localized IBOs allows for a direct connection between intuitive "curly arrows" depictions of reaction mechanisms and quantum chemistry.[77] Key IBOs involved in the reaction mechanism for the formation of $(HC)_3P$ are depicted in Figure 7B. Inspection of the selected IBOs along the intrinsic reaction coordinate clearly shows concerted transformation of the cyclopropenyl π-bond and the phosphorus lone pair into two σ-bonds found in $(HC)_3P$. Additionally, these calculations reveal that the P−Cl

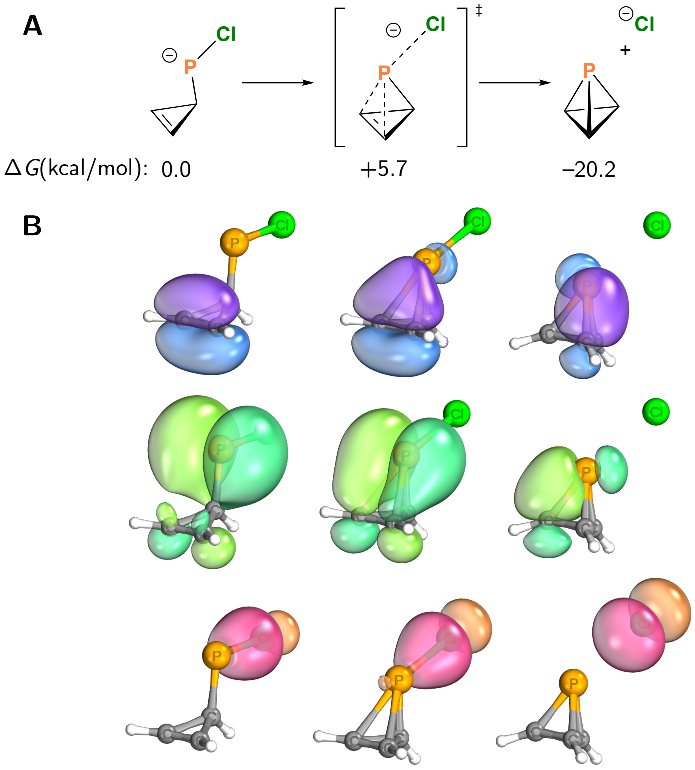

Figure 7: Quantum Chemical Calculations for the Formation of $(HC)_3P$. **A** Depiction of $(HC)_3P$ formation via intramolecular cycloaddition and chloride elimination. Gibbs free enthalpy is reported at 298.15 K. **B** Visualization of electron flow by means of intrinsic bond orbitals (cyclopropenyl π-bond (top), phosphorus lone pair (middle), and P−Cl σ-bond (bottom).

σ-bond transforms into a lone pair of the chloride leaving group.

Conclusion

We have demonstrated that nine hydrogen-hydrogen bonds between neighboring *tert*-butyl groups are essential for the stability of $(^t\text{BuC})_3\text{P}$. The stabilizing contribution associated with each HHB is distance dependent and, on average, each HHB is associated with a stabilization energy of −0.7 kcal/mol due to London dispersion forces. Each HHB is also associated with a destabilizing effect originating from other non-dispersive contributions of the interaction (e.g. Pauli repulsion). Hence, the net stabilizing effect associated with a given HHB is less than −0.7 kcal/mol and the actual value likely lies between −0.25 (for the methane dimer case) and −0.5 kcal/mol (for the isobutane trimer model system). We have also presented a computed mechanism that is consistent with $(^t\mathrm{BuC})_3\mathrm{P}$ formation proceeding via a transiently formed phosphinidenoid species. Analysis of the IBOs along the intrinsic reaction coordinate clearly shows the flow of localized orbitals in this transformation.

Supporting Information Available

XYZ coordinates for all structures and an example procedure for geometry optimization and DLPNO-CCSD(T) LED analysis are in the supplementary materials.

Acknowledgement

Funding: This material is based on research supported by the National Science Foundation under CHE-1955612. **Competing interests:** The authors declare no competing interests.

References

(1) Maier, G.; Pfriem, S.; Schäfer, U.; Matusch, R. Tetra-*tert*-butyltetrahedrane. *Angew. Chem. Int. Ed.* **1978**, *17*, 520–521.

(2) White, E. H.; Winter, R. E. K.; Graeve, R.; Zirngibl, U.; Friend, E. W.; Maskill, H.; Mende, U.; Kreiling, G.; Reisenauer, H. P.; Maier, G. Kleine Ringe, 33: Versuche zur Darstellung von Diphenyltetrahedran. *Chem. Ber.* **1981**, *114*, 3906–3915.

(3) Maier, G.; Reisenauer, H. P. Kleine Ringe, 34: Versuche zur Darstellung von Dimethyltetrahedran. *Chem. Ber.* **1981**, *114*, 3916–3921.

(4) Maier, G.; Schneider, M.; Kreiling, G.; Mayer, W. Kleine Ringe, 35: Versuche zur Darstellung von Tetramethyltetrahedran aus Heterocyclischen Vorstufen. *Chem. Ber.* **1981**, *114*, 3922–3934.

(5) Maier, G.; Reisenauer, H. P. Kleine Ringe, 37: Weitere Versuche zur Matrixisolierung von Tetramethyltetrahedran. *Chem. Ber.* **1981**, *114*, 3959–3964.

(6) Maier, G.; Mayer, W.; Freitag, H.-A.; Reisenauer, H. P.; Askani, R. Kleine Ringe, 36: Versuche zur Darstellung von Tetramethyltetrahedran aus Alicyclischen Vorstufen. *Chem. Ber.* **1981**, *114*, 3935–3958.

(7) Sekiguchi, A.; Tanaka, M. Tetrahedranyllithium: Synthesis, Characterization, and Reactivity. *J. Am. Chem. Soc.* **2003**, *125*, 12684–12685.

(8) Nakamoto, M.; Inagaki, Y.; Nishina, M.; Sekiguchi, A. Perfluoroaryltetrahedranes: Tetrahedranes with Extended σ–π Conjugation. *J. Am. Chem. Soc.* **2009**, *131*, 3172–3173.

(9) Ochiai, T.; Nakamoto, M.; Inagaki, Y.; Sekiguchi, A. Sulfur-Substituted Tetrahedranes. *J. Am. Chem. Soc.* **2011**, *133*, 11504–11507.

(10) Maier, G.; Born, D. Tri-*tert*-butyl(trimethylsilyl)tricyclo[1.1.0.0^{2,4}]-butane−A Second Tetrahedrane Derivative. *Angew. Chem. Int. Ed.* **1989**, *28*, 1050–1052.

(11) Cremer, D.; Kraka, E. Theoretical Determination of Molecular Structure and Conformation. 15. Three-Membered Rings: Bent Bonds, Ring Strain, and Surface Delocalization. *J. Am. Chem. Soc.* **1985**, *107*, 3800–3810.

(12) Cremer, D.; Kraka, E. Theoretical Determination of Molecular Structure and Conformation. 16. Substituted Cyclopropanes - An Electron Density Model of Substituent-Ring Interactions. *J. Am. Chem. Soc.* **1985**, *107*, 3811–3819.

(13) Matta, C. F.; Hernández-Trujillo, J.; Tang, T.-H.; Bader, R. F. W. Hydrogen−Hydrogen Bonding: A Stabilizing Interaction in Molecules and Crystals. *Chem. Eur. J.* **2003**, *9*, 1940–1951.

(14) Bader, R. F. W. *Atoms in Molecules: A Quantum Theory*; Oxford University Press: Oxford, U.K., 1990.

(15) Bader, R. F. W. A Quantum Theory of Molecular Structure and its Applications. *Chem. Rev.* **1991**, *91*, 893–928.

(16) Balci, M.; McKee, M. L.; Schleyer, P. v. R. Theoretical Study of Tetramethyl- and Tetra-*tert*-butyl-Substituted Cyclobutadiene and Tetrahedrane. *J. Phys. Chem. A* **2000**, *104*, 1246–1255.

(17) Schreiner, P. R.; Chernish, L. V.; Gunchenko, P. A.; Tikhonchuk, E. Y.; Hausmann, H.; Serafin, M.; Schlecht, S.; Dahl, J. E. P.; Carlson, R. M. K.; Fokin, A. A. Overcoming Lability of Extremely Long Alkane Carbon−Carbon Bonds Through Dispersion Forces. *Nature* **2011**, *477*, 308–311.

(18) Matta, C. F.; Sadjadi, S. A.; Braden, D. A.; Frenking, G. The Barrier to the Methyl Rotation in *Cis*-2-butene and Its Isomerization Energy to *Trans*-2-butene, Revisited. *J. Comput. Chem.* **2016**, *37*, 143–154.

(19) Cukrowski, I.; Sagan, F.; Mitoraj, M. P. On the Stability of *Cis*- and *Trans*-2-butene Isomers. An Insight Based on the FAMSEC, IQA, and ETS-NOCV Schemes. *J. Comput. Chem.* **2016**, *37*, 2783–2798.

(20) Weinhold, F.; Schleyer, P. v. R.; McKee, W. C. Bay-type H $\cdots$ H "Bonding" in *Cis*-2-butene and Related Species: QTAIM versus NBO Description. *J. Comput. Chem.* **2014**, *35*, 1499–1508.

(21) Poater, J.; Solà, M.; Bickelhaupt, F. M. Hydrogen−Hydrogen Bonding in Planar Biphenyl, Predicted by Atoms-In-Molecules Theory, Does Not Exist. *Chem. Eur. J.* **2006**, *12*, 2889–2895.

(22) Eskandari, K.; Van Alsenoy, C. Hydrogen−Hydrogen Interaction in Planar Biphenyl: A Theoretical Study Based on the Interacting Quantum Atoms and Hirshfeld Atomic Energy Partitioning Methods. *J. Comput. Chem.* **2014**, *35*, 1883–1889.

(23) Bader, R. F. W. Pauli Repulsions Exist Only in the Eye of the Beholder. *Chem. Eur. J.* **2006**, *12*, 2896–2901.

(24) Hernández-Trujillo, J.; Matta, C. F. Hydrogen−Hydrogen Bonding in Biphenyl Revisited. *Struct. Chem.* **2007**, *18*, 849–857.

(25) Popelier, P. L. A.; Maxwell, P. I.; Thacker, J. C. R.; Alkorta, I. A Relative Energy Gradient (REG) Study of the Planar and Perpendicular Torsional Energy Barriers in Biphenyl. *Theor. Chem. Acc.* **2018**, *138*, 12.

(26) Mitoraj, M. P.; Sagan, F.; Szczepanik, D. W.; Lange, J. H. d.; Ptaszek, A. L.; Niekerk, D. M. E. v.; Cukrowski, I. Origin of Hydrocarbons Stability from a Computational Perspective: A Case Study of Ortho-Xylene Isomers. *ChemPhysChem* **2020**, *21*, 494–502.

(27) Sagan, F.; Mariusz, M. P. *Transition Metals in Coordination Environments: Computational Chemistry and Catalysis Viewpoints*; Springer International Publishing: Cham, Switzerland, 2019; p 65–89.

(28) Echeverría, J.; Aullón, G.; Danovich, D.; Shaik, S.; Alvarez, S. Dihydrogen Contacts in Alkanes are Subtle but Not Faint. *Nat. Chem.* **2011**, *3*, 323–330.

(29) Danovich, D.; Shaik, S.; Neese, F.; Echeverría, J.; Aullón, G.; Alvarez, S. Understanding the Nature of the CH$\cdots$HC Interactions in Alkanes. *J. Chem. Theory Comput.* **2013**, *9*, 1977–1991.

(30) Rösel, S.; Quanz, H.; Logemann, C.; Becker, J.; Mossou, E.; Cañadillas-Delgado, L.;

Caldeweyher, E.; Grimme, S.; Schreiner, P. R. London Dispersion Enables the Shortest Intermolecular Hydrocarbon H···H Contact. *J. Am. Chem. Soc.* **2017**, *139*, 7428–7431.

(31) Monteiro, N. K. V.; Firme, C. L. Hydrogen−Hydrogen Bonds in Highly Branched Alkanes and in Alkane Complexes: A DFT, Ab Initio, QTAIM, and ELF Study. *J. Phys. Chem. A* **2014**, *118*, 1730–1740.

(32) J. Wolstenholme, D.; L. Dobson, J.; Sean McGrady, G. Homopolar Dihydrogen Bonding in Main Group Hydrides: Discovery, Consequences, and Applications. *Dalton Trans.* **2015**, *44*, 9718–9731.

(33) Echeverría, J.; Aullón, G.; Alvarez, S. Dihydrogen Intermolecular Contacts in Group 13 Compounds: H···H or E···H (E = B, Al, Ga) Interactions? *Dalton Trans.* **2017**, *46*, 2844–2854.

(34) Echeverría, J.; Aullón, G.; Alvarez, S. Intermolecular Interactions in Group 14 Hydrides: Beyond C−H···H−C Contacts. *Int. J. Quantum Chem.* **2017**, *117*, e25432.

(35) Wolstenholme, D. J.; Titah, J. T.; Che, F. N.; Traboulsee, K. T.; Flogeras, J.; McGrady, G. S. Homopolar Dihydrogen Bonding in Alkali-Metal Amidoboranes and Its Implications for Hydrogen Storage. *J. Am. Chem. Soc.* **2011**, *133*, 16598–16604.

(36) Wolstenholme, D. J.; Flogeras, J.; Che, F. N.; Decken, A.; McGrady, G. S. Homopolar Dihydrogen Bonding in Alkali Metal Amidoboranes: Crystal Engineering of Low-Dimensional Molecular Materials. *J. Am. Chem. Soc.* **2013**, *135*, 2439–2442.

(37) Sagan, F.; Filas, R.; Mitoraj, M. P. Non-Covalent Interactions in Hydrogen Storage Materials $LiN(CH_3)_2BH_3$ and $KN(CH_3)_2BH_3$. *Crystals* **2016**, *6*, 28.

(38) Safin, D. A.; Babashkina, M. G.; Robeyns, K.; Mitoraj, M. P.; Kubisiak, P.; Garcia, Y. Influence of the Homopolar Dihydrogen Bonding C−H···H−C on Coordination Geometry: Experimental and Theoretical Studies. *Chem. Eur. J.* **2015**, *21*, 16679–16687.

(39) Riu, M.-L. Y.; Jones, R. L.; Transue, W. J.; Müller, P.; Cummins, C. C. Isolation of an Elusive Phosphatetrahedrane. *Sci. Adv.* **2020**, *6*, eaaz3168.

(40) Hierlmeier, G.; Coburger, P.; Bodensteiner, M.; Wolf, R. Di-*tert*-butyldiphosphatetrahedrane: Catalytic Synthesis of the Elusive Phosphaalkyne Dimer. *Angew. Chem. Int. Ed.* **2019**, *58*, 16918–16922.

(41) Kutzelnigg, W. Chemical Bonding in Higher Main Group Elements. *Angew. Chem. Int. Ed.* **1984**, *23*, 272–295.

(42) Wolf, M. E.; Doty, E. A.; Turney, J. M.; Schaefer III, H. F. Highly Strained $Pn(CH)_3$ ($Pn = N, P, As, Sb, Bi$) Tetrahedranes: Theoretical Characterization. *J. Phys. Chem. A* **2021**, *125*, 2612–2621.

(43) Bistoni, G. Finding Chemical Concepts in the Hilbert Space: Coupled Cluster Analyses of Noncovalent Interactions. *WIREs Comput. Mol. Sci.* **2020**, *10*, e1442.

(44) Pérez-Jordá, J. M.; Becke, A. A Density-Functional Study of van der Waals Forces: Rare Gas Diatomics. *Chem. Phys. Lett.* **1995**, *233*, 134–137.

(45) Kristyán, S.; Pulay, P. Can (Semi)local Density Functional Theory Account for the London Dispersion Forces? *Chem. Phys. Lett.* **1994**, *229*, 175–180.

(46) Grimme, S.; Antony, J.; Ehrlich, S.; Krieg, H. A Consistent and Accurate *Ab Initio* Parametrization of Density Functional Dispersion Correction (DFT-D) for the 94 Elements H-Pu. *J. Chem. Phys.* **2010**, *132*, 154104.

(47) Bistoni, G.; Auer, A. A.; Neese, F. Understanding the Role of Dispersion in Frustrated Lewis Pairs and Classical Lewis Adducts: A Domain-Based Local Pair Natural Orbital Coupled Cluster Study. *Chem. Eur. J.* **2017**, *23*, 865–873.

(48) Riplinger, C.; Sandhoefer, B.; Hansen, A.; Neese, F. Natural Triple Excitations in Local

Coupled Cluster Calculations with Pair Natural Orbitals. *J. Chem. Phys.* **2013**, *139*, 134101.

(49) Riplinger, C.; Pinski, P.; Becker, U.; Valeev, E. F.; Neese, F. Sparse Maps—A Systematic Infrastructure for Reduced-Scaling Electronic Structure Methods. II. Linear Scaling Domain Based Pair Natural Orbital Coupled Cluster Theory. *J. Chem. Phys.* **2016**, *144*, 024109.

(50) Schneider, W. B.; Bistoni, G.; Sparta, M.; Saitow, M.; Riplinger, C.; Auer, A. A.; Neese, F. Decomposition of Intermolecular Interaction Energies within the Local Pair Natural Orbital Coupled Cluster Framework. *J. Chem. Theory Comput.* **2016**, *12*, 4778–4792.

(51) Altun, A.; Neese, F.; Bistoni, G. Effect of Electron Correlation on Intermolecular Interactions: A Pair Natural Orbitals Coupled Cluster Based Local Energy Decomposition Study. *J. Chem. Theory Comput.* **2019**, *15*, 215–228.

(52) Altun, A.; Saitow, M.; Neese, F.; Bistoni, G. Local Energy Decomposition of Open-Shell Molecular Systems in the Domain-Based Local Pair Natural Orbital Coupled Cluster Framework. *J. Chem. Theory Comput.* **2019**, *15*, 1616–1632.

(53) Neese, F. The ORCA Program System. *WIREs Comput. Mol. Sci.* **2012**, *2*, 73–78.

(54) Neese, F. Software Update: The ORCA Program System, Version 4.0. *WIREs Comput. Mol. Sci.* **2018**, *8*, e1327.

(55) Tao, J.; Perdew, J. P.; Staroverov, V. N.; Scuseria, G. E. Climbing the Density Functional Ladder: Nonempirical Meta–Generalized Gradient Approximation Designed for Molecules and Solids. *Phys. Rev. Lett.* **2003**, *91*, 146401.

(56) Weigend, F.; Ahlrichs, R. Balanced Basis Sets of Split Valence, Triple Zeta Valence

and Quadruple Zeta Valence Quality for H to Rn: Design and Assessment of Accuracy. *Phys. Chem. Chem. Phys.* **2005**, *7*, 3297–3305.

(57) Weigend, F. Accurate Coulomb-Fitting Basis Sets for H to Rn. *Phys. Chem. Chem. Phys.* **2006**, *8*, 1057–1065.

(58) Becke, A. D.; Johnson, E. R. A Density-Functional Model of the Dispersion Interaction. *J. Chem. Phys.* **2005**, *123*, 154101.

(59) Grimme, S.; Ehrlich, S.; Goerigk, L. Effect of the Damping Function in Dispersion Corrected Density Functional Theory. *J. Comput. Chem.* **2011**, *32*, 1456–1465.

(60) Barone, V.; Cossi, M. Quantum Calculation of Molecular Energies and Energy Gradients in Solution by a Conductor Solvent Model. *J. Phys. Chem. A* **1998**, *102*, 1995–2001.

(61) Guo, Y.; Riplinger, C.; Becker, U.; Liakos, D. G.; Minenkov, Y.; Cavallo, L.; Neese, F. Communication: An Improved Linear Scaling Perturbative Triples Correction for the Domain Based Local Pair-Natural Orbital Cased Singles and Doubles Coupled Cluster Method [DLPNO-CCSD(T)]. *J. Chem. Phys.* **2018**, *148*, 011101.

(62) Neese, F.; Hansen, A.; Liakos, D. G. Efficient and Accurate Approximations to the Local Coupled Cluster Singles Doubles Method using a Truncated Pair Natural Orbital Basis. *J. Chem. Phys.* **2009**, *131*, 064103.

(63) Kendall, R. A.; Dunning, T. H.; Harrison, R. J. Electron Affinities of the First-Row Atoms Revisited. Systematic Basis Sets and Wave Functions. *J. Chem. Phys.* **1992**, *96*, 6796–6806.

(64) Lu, Q.; Neese, F.; Bistoni, G. London Dispersion Effects in the Coordination and Activation of Alkanes in σ-Complexes: A Local Energy Decomposition Study. *Phys. Chem. Chem. Phys.* **2019**, *21*, 11569–11577.

(65) Knizia, G. Intrinsic Atomic Orbitals: An Unbiased Bridge Between Quantum Theory and Chemical Concepts. *J. Chem. Theory Comput.* **2013**, *9*, 4834–4843.

(66) Knizia, G. *Iboview.* `http://www.iboview.org/` (accessed 08/02/2020).

(67) Wagner, J. P.; Schreiner, P. R. London Dispersion in Molecular Chemistry−Reconsidering Steric Effects. *Angew. Chem. Int. Ed.* **2015**, *54*, 12274–12296.

(68) Liptrot, D. J.; Power, P. P. London Dispersion Forces in Sterically Crowded Inorganic and Organometallic Molecules. *Nat. Rev. Chem.* **2017**, *1*, 0004.

(69) Hounshell, W. D.; Mislow, K. Tetra-*tert*-butyltetrahedrane has T Symmetry. *Tetrahedron Lett.* **1979**, *20*, 1205–1208.

(70) Mitoraj, M. P.; Sagan, F.; Babashkina, M. G.; Isaev, A. Y.; Chichigina, Y. M.; Safin, D. A. *N*-Thiophosphorylthioureas RNHC(S)NHP(S)(O*i*Pr)$_2$ as an Excellent Platform for Studying the Synergy between Hydrogen-Hydrogen Bonding and Other Families of Non-Covalent Interactions. *Eur. J. Org. Chem.* **2019**, *2019*, 493–503.

(71) Blanco, M. A.; Martín Pendás, A.; Francisco, E. Interacting Quantum Atoms: A Correlated Energy Decomposition Scheme Based on the Quantum Theory of Atoms in Molecules. *J. Chem. Theory Comput.* **2005**, *1*, 1096–1109.

(72) Cukrowski, I. IQA-Embedded Fragment Attributed Molecular System Energy Change in Exploring Intramolecular Interactions. *Comput. Theor. Chem.* **2015**, *1066*, 62–75.

(73) Wuttke, A.; Mata, R. A. Visualizing Dispersion Interactions Through the Use of Local Orbital Spaces. *J. Comput. Chem.* **2017**, *38*, 15–23.

(74) Boche, G.; Lohrenz, J. C. W. The Electrophilic Nature of Carbenoids, Nitrenoids, and Oxenoids. *Chem. Rev.* **2001**, *101*, 697–756.

(75) Özbolat, A.; von Frantzius, G.; Pérez, J. M.; Nieger, M.; Streubel, R. Strong Evidence for a Transient Phosphinidenoid Complex. *Angew. Chem. Int. Ed.* **2007**, *46*, 9327–9330.

(76) Schmer, A.; Junker, P.; Espinosa Ferao, A.; Streubel, R. M/X Phosphinidenoid Metal Complex Chemistry. *Acc. Chem. Res.* **2021**, *54*, 1754–1765.

(77) Knizia, G.; Klein, J. E. M. N. Electron Flow in Reaction Mechanisms—Revealed from First Principles. *Angew. Chem. Int. Ed.* **2015**, *54*, 5518–5522.

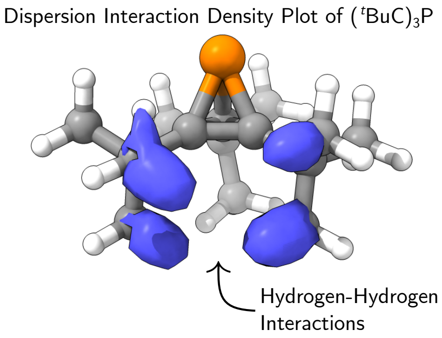
Dispersion Interaction Density Plot of (^{t}BuC)$_3$P
Hydrogen-Hydrogen Interactions

TOC Graphic